J. Fluid Mech. (1988), *vol.* 186, *pp.* 63–84
Printed in Great Britain

Excitation of instability waves in free shear layers. Part 2. Experiments

By D. W. BECHERT AND B. STAHL
DFVLR, Abteilung Turbulenzforschung, Müller-Breslau-Straße 8, 1000 Berlin-West 12, West Germany

(Received 17 September 1985 and in revised form 20 March 1987)

The acoustical excitation of shear layers is investigated experimentally. Acoustical excitation causes, for example, the so-called 'orderly structures' in shear layers and jets. Also, the deviations in the spreading rate between different turbulent-shear-layer experiments are due to the same excitation mechanism. The present investigations focus on measurements in the linear interaction region close to the edge from which the shear layer is shed. We report on two sets of experiments (Houston 1981 and Berlin 1983/84). The measurements have been carried out with laminar shear layers in air using hot-wire anemometers and microphones. The agreement between these measurements and the theory is good. Even details of the fluctuating flow field correspond to theoretical predictions, such as the local occurrence of negative phase speeds.

1. Introduction

The fact that sound waves cause wavelike perturbations and orderly vortex formations in shear layers and jets has been known for at least one hundred years (see Leconte 1858; Tyndall 1867). Excellent photographs of shear layers demonstrating the evolution of vortices have even been available for more than fifty years, see figure 1. Observations on excited jets led to the development of the stability theory of flows by Lord Kelvin, von Helmholtz and Lord Rayleigh. The interest of theoreticians in the following century was concentrated on determining the limits of the stability of flows and on the evolution of the instability waves including their nonlinear development leading to turbulence.

On the other hand, little attention had been paid to the understanding of the initial observations, i.e. that instability waves in shear layers are tied to acoustical waves. During the last decade, it was demonstrated that turbulent flows can also be dominated by instability waves and the subsequent evolution of turbulent vortices (Crow & Champagne 1971). Also, the significance of acoustic excitation became evident in turbulent shear flows, as it was in the analogous case of laminar shear layers (Dziomba & Fiedler 1985; Gutmark & Ho 1983). Moreover, the observation that the broadband noise emission of turbulent jets can be enhanced by acoustical tone excitation (Bechert & Pfizenmaier 1975*a*; Moore 1977; Deneuville & Jaques 1977) has increased interest in the forcing mechanism of instability waves. Thus, a small number of theoretical papers on acoustical shear-layer excitation has emerged in the past ten years (Crighton & Leppington 1974; Bechert & Michel 1975; Möhring 1975; Rienstra 1979). Unfortunately, these papers did not produce results that were easily verifiable by experimentalists. In addition, there was no guideline on what the relevant quantities to be measured were, and how to proceed in such an experiment.

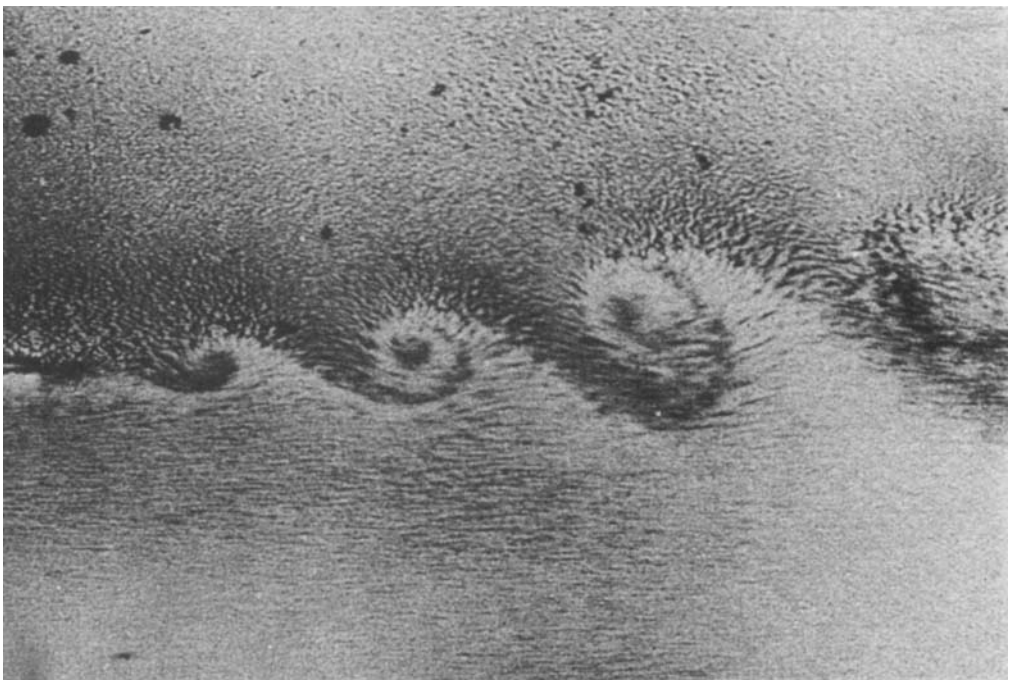

FIGURE 1. Roll-up process in a shear layer. Photograph taken by F. Michel (1932).

One of the present authors has attempted to produce the necessary theoretical data in a preceding report (Bechert 1982; and Part 1 of this paper, Bechert 1988, hereinafter referred to as I). The present experimental investigation aims at verifying this theoretical material.

We provide here two sets of data obtained in different institutes. The first set was obtained in 1981 by D. W. Bechert at the University of Houston. However, it was suspected that these data might have been slightly contaminated by systematic errors caused, for example, by: (i) overshoot of the mean velocity profile at the shear layer; (ii) too high vibration levels in the facility which caused problems with the vibration sensitivity of the microphones; (iii) partly unreliable electronic instruments, such as a beat frequency oscillator, which did not keep the excitation frequency sufficiently constant.

Subsequently, the major possible error sources were scrutinized and it was concluded that the Houston data were at least of value in suggesting that the theory is correct. Thus, some data were published (Bechert 1983).

A second facility was then established in Berlin. The new data obtained by the present authors were much more reliable and reproducible, but it turned out that only a *little* of the Houston data had to be rejected, and none that had been published. In hindsight, it might appear that we were overscrupulous in carrying out the experiment twice. However, the issue of shear-layer excitation is so confused, that it seemed worthwhile to have this double effort to solve the problem.

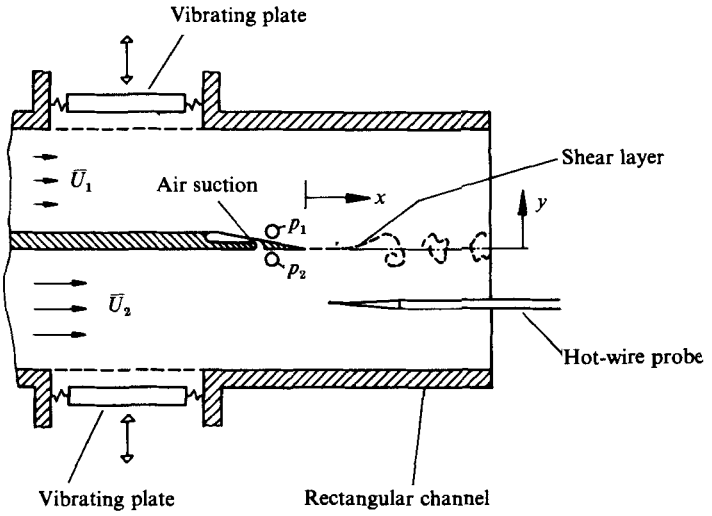

FIGURE 2. Experimental arrangement.

2. A brief description of the facility

Figure 2 shows the test section of the experimental set-up. The splitter plate in the centre of a rectangular channel separates the mean flow region ($\bar{U} = \bar{U}_2$ at $y < 0$) from a region of very slow entrainment flow ($\bar{U}_1 \approx 0.1\bar{U}_2$ at $y > 0$). The initial shear-layer thickness can be controlled by boundary-layer suction through a slit in the splitter plate near the plate edge.

The excitation is provided by two vibrating plates driven electromagnetically and adjusted in antiphase so that a surging motion around the edge of the splitter plate is produced. The magnitude of the excitation field is measured by two microphones, one on each side of the splitter plate. The pressure difference $p_1 - p_2 = \Delta p_{12}$ is a direct measure of the acoustic excitation.

In order to prevent any effects of the suction slit on the sound field, the oscillating flow through the slit can be compensated acoustically by a piston speaker in the suction duct. This piston speaker can be adjusted in magnitude and phase so that a zero oscillating flow condition through the slit is achieved. This is checked by a second hot-wire probe (not shown in figure 2) inserted into the slit. In this way, the suction slit can be sealed acoustically.

Although this brief description is sufficient to understand the measured data in the following sections, to appreciate how comparatively involved these measurements really are, the interested reader should see the more detailed description of the experimental apparatus in our previous report (Bechert & Stahl 1984). The flavour of the project can be appreciated much better if one knows explicitly where we used, for example, ladies' stockings, coffee filters, an empty barrel, a garden hose and a vacuum cleaner.

3. Mean flow field

The data in this investigation were taken under 4 different mean flow conditions, namely a mean flow velocity of 6 m/s or 12 m/s with boundary-layer suction† off or

† Suction rate: 28.3 l/min (Houston) and 34.0 l/min (Berlin). The rate was the same for the 6 m/s and 12 m/s mean velocity. The splitter plate breadth was 100 mm in both facilities.

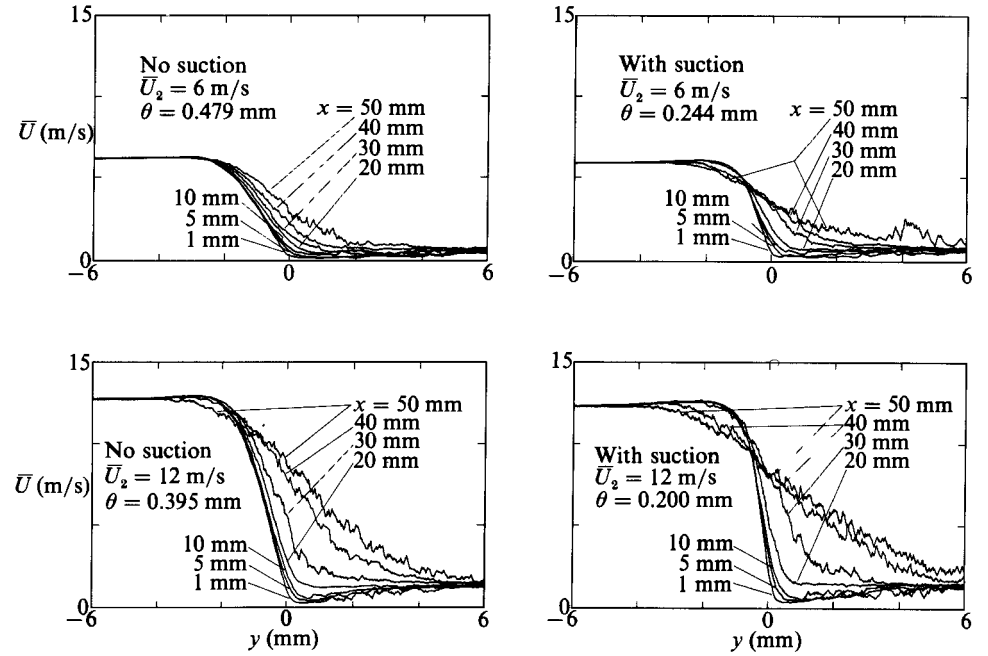

FIGURE 3. Mean flow distribution (Houston 1981 experiment).

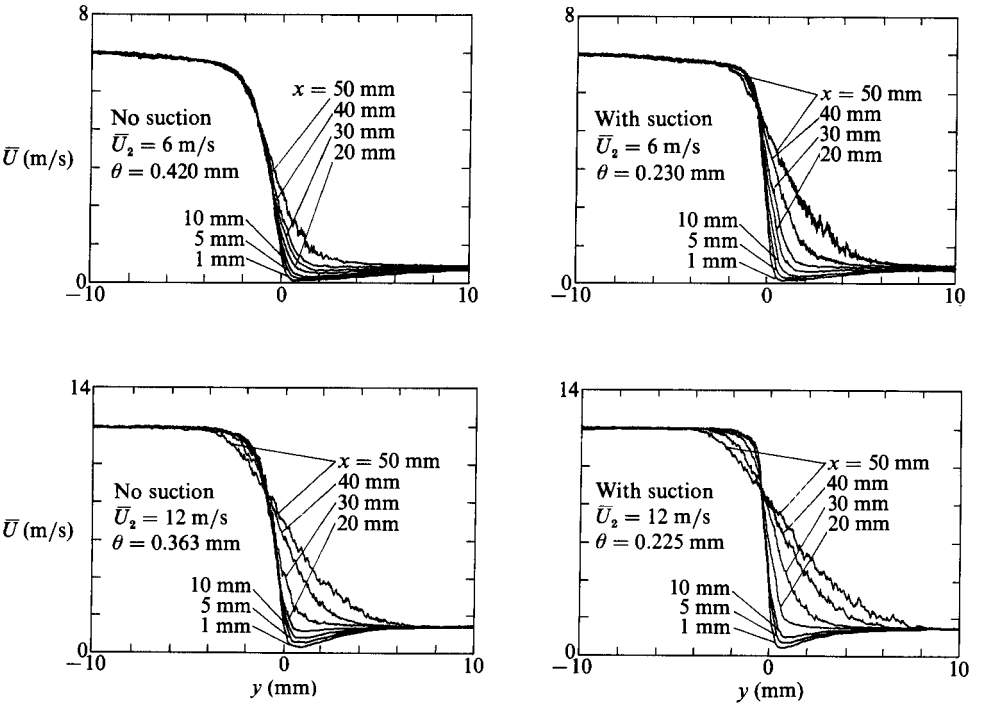

FIGURE 4. Mean flow distribution (Berlin 1983/84 experiment).

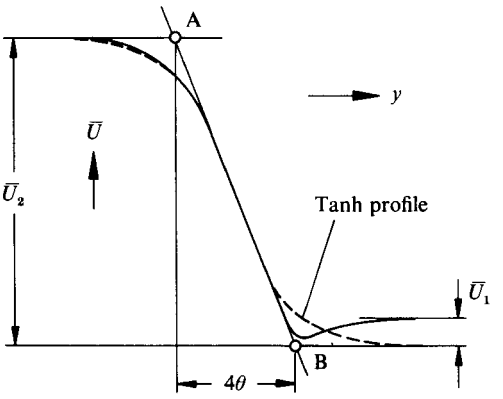

FIGURE 5. On the definition of θ.

on. For each data set, Houston 1981, and Berlin 1983/84, the mean velocity distributions were measured (see figures 3 and 4). The location $y = 0$ in figures 3 and 4 refers to the location of the sharp trailing edge of the splitter plate.

The Houston data show a little overshoot in the potential-flow region, which is due to an interaction between screen and nozzle (see also Bechert & Stahl 1984). If we consider the differences between measurements without and with boundary-layer suction, we see that (i) the boundary-layer suction indeed decreases the initial shear-layer thickness effectively, and (ii) on the other hand, farther downstream, the shear-layer spreading rate is increased. Thus, the boundary-layer suction produces a smaller shear-layer thickness only over a certain downstream distance. In addition, we see that it is hard to define a meaningful shear-layer thickness θ. The situation becomes even more complex if we consider the splitter-plate wake, which is particularly visible for the Berlin measurements (where we have no turbulent separation at the splitter plate as in the Houston data). A definition (see also figure 5) like, for example,

$$\theta_1 = \int_{-\infty}^{+\infty} \frac{\bar{U}_{(y)} - \bar{U}_1}{\bar{U}_2 - \bar{U}_1} \left(1 - \frac{\bar{U}_{(y)} - \bar{U}_1}{\bar{U}_2 - \bar{U}_1}\right) \mathrm{d}y, \tag{1}$$

would lead, with the present data, to a momentum thickness that always varies with x, whereas we would prefer to have a simple reference quantity for the shear-layer thickness. A quantity, however, which does not vary very much within the first 15 mm downstream of the plate edge is the *slope* of the mean velocity profile. Therefore, we use the following definition which, admittedly, is not very sophisticated but appeared to be suitable (see figure 5):

(i) we determine the slope of the initial profile at, say, $x = 1$ mm, where the slope is still identical with that of the plate boundary layer; (ii) we replace the real velocity profile with a hyperbolic tangent profile of the same slope; (iii) we determine the points A and B where the slope line intersects the lines $\bar{U} = 0$ and $\bar{U} = \bar{U}_2$, and we determine the horizontal distance of the two points A and B. For a hyperbolic tangent profile this distance would be 4 times the momentum thickness θ. So we divide the horizontal distance AB by four.

We take this latter artificial momentum thickness θ as our reference quantity. This reference quantity is not too dissimilar to Freymuth's (1966) θ_m. Readers who are not

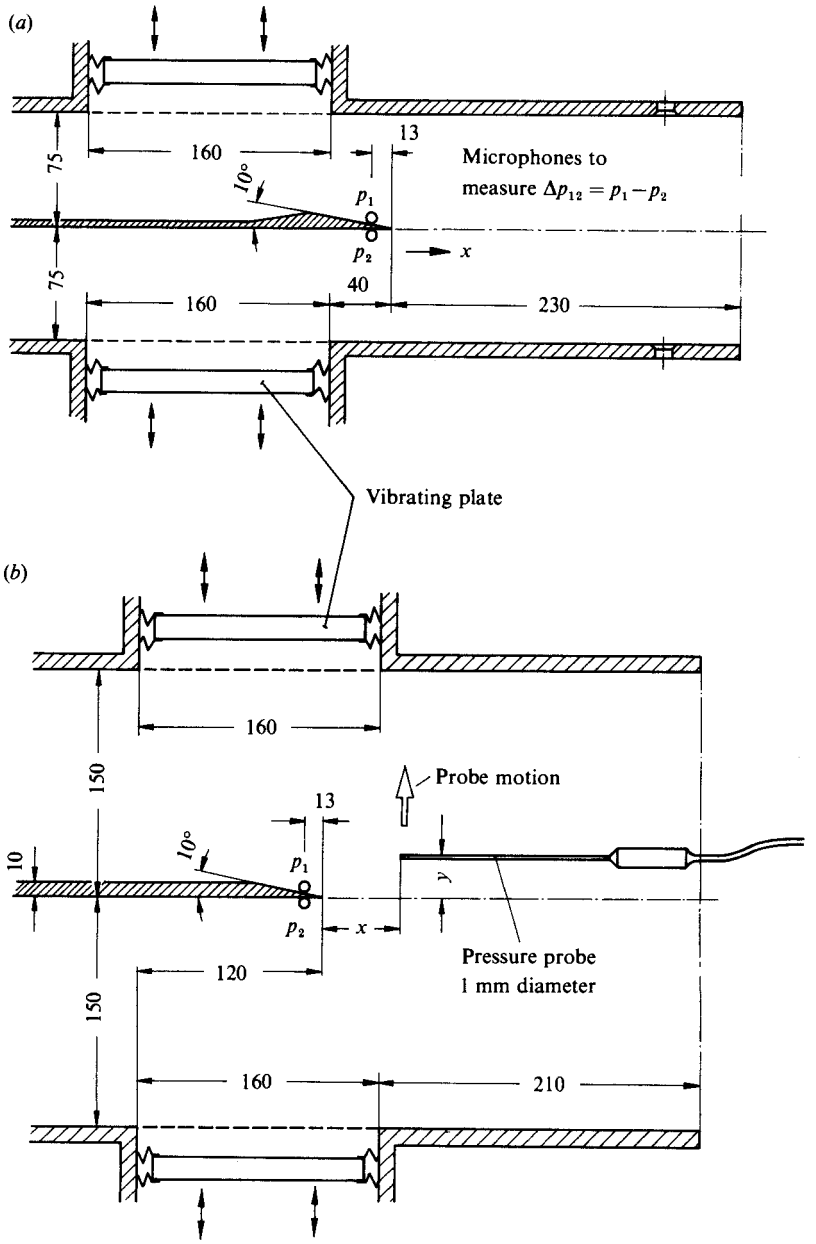

FIGURE 6. Configuration of the test sections. (*a*) Houston 1981; (*b*) Berlin 1983/84. Dimensions in mm.

satisfied with this crude definition of the momentum thickness θ might redefine it with the data of figures 3 and 4.

4. Excitation sound field

The geometry of our test sections is shown in figure 6. The shear layer is excited by two vibrating plates which are driven by electromagnetic loudspeaker systems. In

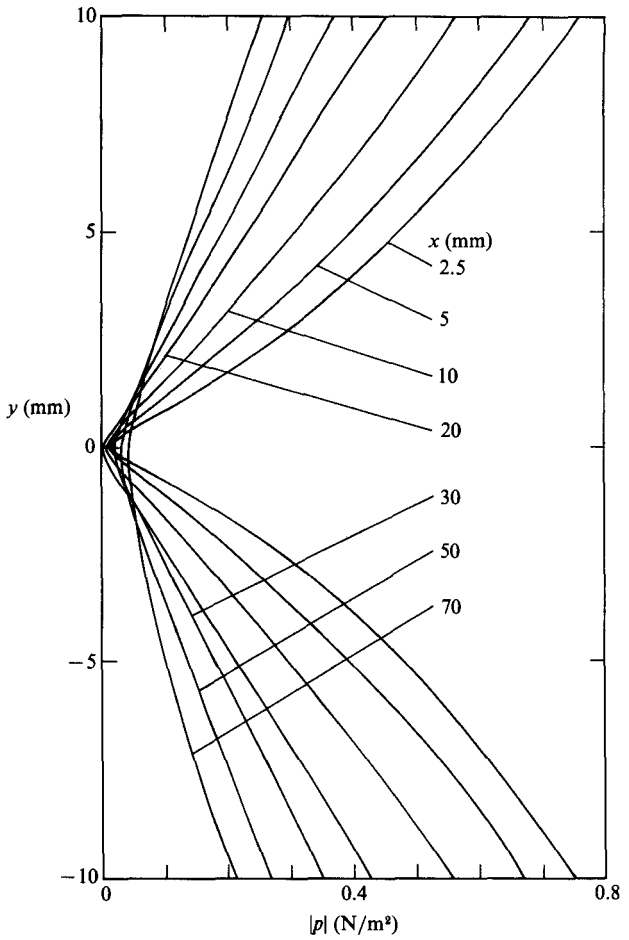

FIGURE 7. Fluctuating pressure distribution in the test section without flow. Data taken at $f = 200$ Hz in the Berlin facility. x is the distance downstream of the trailing edge of the splitter plate.

both sets of data (Houston 1981 and Berlin 1983/84) the same vibrating plates were used. The vibrating plates operate in antiphase, i.e. both are moving up and down simultaneously and produce a surging flow around the splitter-plate edge. The boundary-layer suction slit in the splitter plate is not drawn in figure 6, and it is, in any case, sealed during the excitation-field measurements. To the left-hand side of the test sections a nozzle is connected from which the mean flow comes. The region below the symmetry line contains the stream of high velocity $\bar{U}_2$. During the excitation-field pressure measurements, however, the mean flow is switched off.

Before the data are collected, the pressure probe is moved to the symmetry line $y = 0$ at a distance not too close (about $x = 10$ mm) to the edge of the splitter plate. The vibrating plates are operated at the frequency of the subsequent shear-layer experiment. Then, the phase and magnitude of the vibrating plates are adjusted so that we obtain zero pressure at the probe location.

With this antisymmetrical adjustment we collect the excitation-field data. A typical data plot can be seen in figure 7. The modulus of the pressure $|p|$ is plotted linearly on the horizontal axis and the vertical distance y from the symmetry line in the test section corresponds to the vertical axis. The phase of p shifts by 180° if we

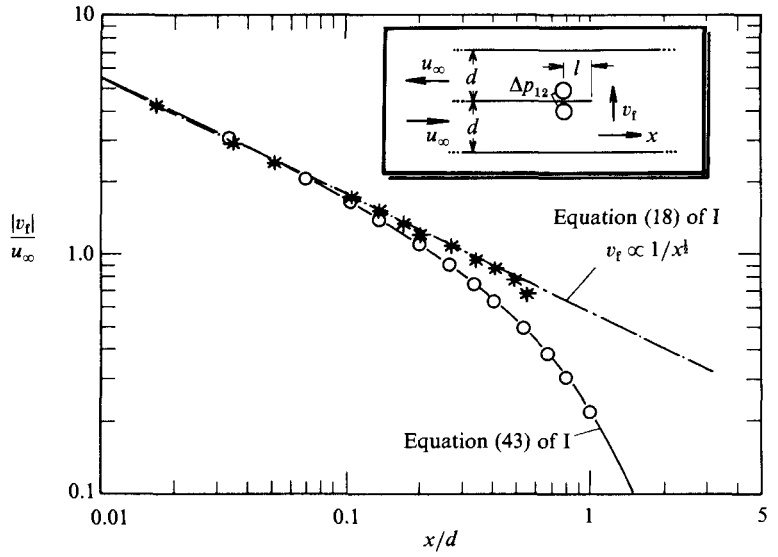

FIGURE 8. Fluctuating velocity distribution of the forcing field v_f. Comparison of experimental data under different configurations (see figure 6) with theory, with channel of width $2d$. Reference velocity: $u_\infty = (|\Delta p_{12}|/4\rho\omega l^{\frac{1}{2}})(\pi/d)^{\frac{1}{2}}$. Houston 1981: ○, $f = 100$ Hz. Berlin 1983/84: ×, $f = 100$ Hz; +, $f = 200$ Hz.

move the probe from negative y to positive y, so we indeed have an antisymmetric pressure field. Theoretically, the pressures for the various x should all be zero at $y = 0$. Since the facility is not completely symmetrical, this occurs exactly only at the location where the zero adjustment has been made.

A graphical evaluation of the forcing velocity v_f from the pressure data using the Euler equations is shown in figure 8. The data from the Houston facility (see figure 6*a*) follow exactly the prediction of I (equation (43)).† The vibrating plates of the Berlin facility are located farther downstream. This produces a v_f distribution which follows more closely the desired $1/x^{\frac{1}{2}}$ distribution of an 'infinite' facility. In the regime where the shear-layer interaction data are collected, up to $x = 30$ mm, the Berlin facility shows no deviations from the $1/x^{\frac{1}{2}}$ law.

For the case with flow, the excitation level Δp_{12} is sometimes not maintained. In particular, in the Berlin facility the excitation field is sometimes slightly changed due to impedance changes of the nozzle with flow. The evaluation of the data is based, however, on a direct measurement of Δp_{12} (with flow) by microphones inserted flush to the sidewall. This requires that the sound field is strictly two-dimensional, which has been checked carefully. In fact, the proper adjustment of the sound field is not crucial for the shear-layer excitation experiments. Nevertheless, it is dependent on an accurate determination of $\Delta \boldsymbol{p}_{12} = \boldsymbol{p}_1 - \boldsymbol{p}_2$, which is a difference of two quantities that can have arbitrary phase angles. This difference can be measured electronically with two microphones. For better accuracy, however, one microphone is used which is moved from location '1' to location '2'. In both locations, the magnitudes p_1, p_2 and phases ϕ_1, ϕ_2 relative to an arbitrary reference phase are measured. $|\Delta p_{12}|$ is then determined by vector subtraction, namely

$$|\Delta p_{12}| = [|p_1|^2 + |p_2|^2 - 2|p_1||p_2|\cos(\phi_1 - \phi_2)]^{\frac{1}{2}}. \tag{2}$$

† The data are normalized with the velocity u_∞ occurring theoretically far upstream in the channel. (For a derivation of u_∞ see Bechert 1982.)

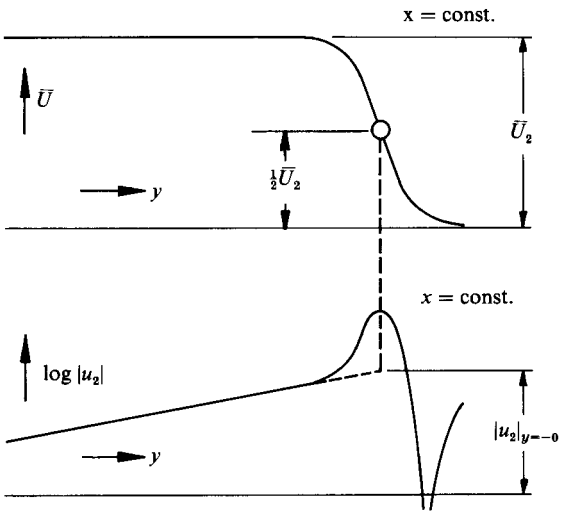

FIGURE 9. Mean flow velocity profile and logarithmic plot of the fluctuating velocity $|u_2|$ with extrapolation.

For those not acquainted with the logarithmic dB scale of pressures, the conversion from pressure in dB from sound-level meters, to pressures in N/m^2, as we use them here, is

$$p(N/m^2) = 2 \times 10^{-5} \times 10^{(p(dB)/20)}. \tag{3}$$

5. Interaction measurements

5.1. *Extrapolated field data*

The shear layer is excited at one single frequency. In order to suppress the background noise the velocity signal taken with a hot-wire probe is filtered at the same frequency. We shall show here data for $|\tilde{u}_2|_{y=0}$, extrapolated from measurements outside the shear layer in the potential flow. The procedure is as follows: We plot the data measured in the potential field outside the shear layer on logarithmic paper and extrapolate linearly towards the centre of the shear layer (see figure 9). This procedure should work at least for locations farther downstream, where we expect an exponential decay of the instability waves in the y-direction. The technique is useful to plot out numerous data, but it has also its limitations, as will become evident if we consider the numerically calculated distributions of $|\tilde{u}_2|$. Such data are provided in I, figure 2, which shows that an extrapolation for $y = -0$ at small $\tilde{x}$ produces too low values of $|\tilde{u}_2|_{(y=-0)}$. At sufficient distance, say at $\tilde{x} > 0.5$, the extrapolation is valid, though. A direct comparison between measurements and computed values, as in figure 2 of I, is more conclusive and will also be carried out for one series of data.

Figures 10 and 11 show the data taken in Houston† and in Berlin. The Houston data show a trend to lower values for small Strouhal numbers which can be explained as a lower excitation due to a narrower test section. This trend is well predicted by

† The data shown in figure 10 are similar to those in Bechert (1983). The Strouhal numbers, however, are slightly different for two reasons. First, the mean velocity data to determine the momentum thickness θ of the shear layer have been revised in order to avoid such data where probe interference had changed the measurement of the shear-layer profile. Secondly, the momentum thickness θ is now chosen according to the procedure suggested in §3.

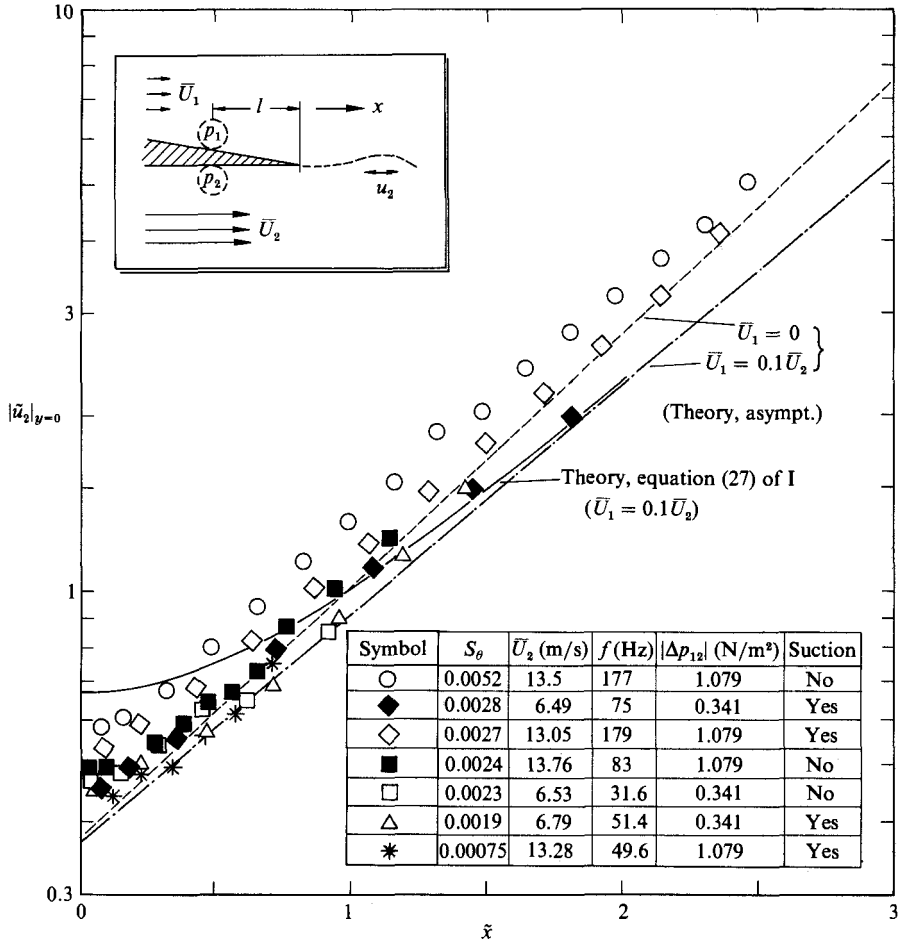

Symbol	S_θ	$\bar{U}_2$ (m/s)	f(Hz)	$\lvert\Delta p_{12}\rvert$ (N/m²)	Suction
○	0.0052	13.5	177	1.079	No
◆	0.0028	6.49	75	0.341	Yes
◇	0.0027	13.05	179	1.079	Yes
■	0.0024	13.76	83	1.079	No
□	0.0023	6.53	31.6	0.341	No
△	0.0019	6.79	51.4	0.341	Yes
✳	0.00075	13.28	49.6	1.079	Yes

FIGURE 10. Shear-layer excitation (data: Houston 1981). Experiments with finite shear-layer thickness θ compared with theory for an infinitesimally thin shear layer. The diagram shows the dependence of the fluctuation velocity $|\tilde{u}_2|_{y=0}$ on the downstream distance $\tilde{x}$ for various Strouhal numbers $S_\theta = f\theta/\bar{U}_2$.

equation (44) of I. For higher Strouhal numbers we see a general trend to increasing fluctuation levels well above the theoretical prediction. Significant deviations begin at $S_\theta \approx 0.005$, as expected (see I). For comparison, we show equation (27) of I, the theoretical prediction for $\bar{U}_1 = 0.1\bar{U}_2$, as well as its asymptote for large $\tilde{x}$. We have also drawn the asymptote for $\bar{U}_1 = 0$, the one-stream case (equation (23) of I), which is the asymptotic form of equation (19) of I. This comparison shows clearly the influence of the second stream. The real situation, however, is more complex. In the mean flow profiles we see a wake caused by the splitter plate which is filled gradually for increasing downstream distance x (see §3 on the mean flow field). Therefore, it makes sense to plot both theoretical curves.

5.2. *Direct comparison of the field data*

For one comparatively low Strouhal number, $S_\theta = 0.0023$, figures 12 and 13 show measured and computed $|u_2|$-field data. In the diagrams in each figure we see a plot of the mean velocity distribution $\bar{U}$ and, with another velocity scale, a (jagged) plot

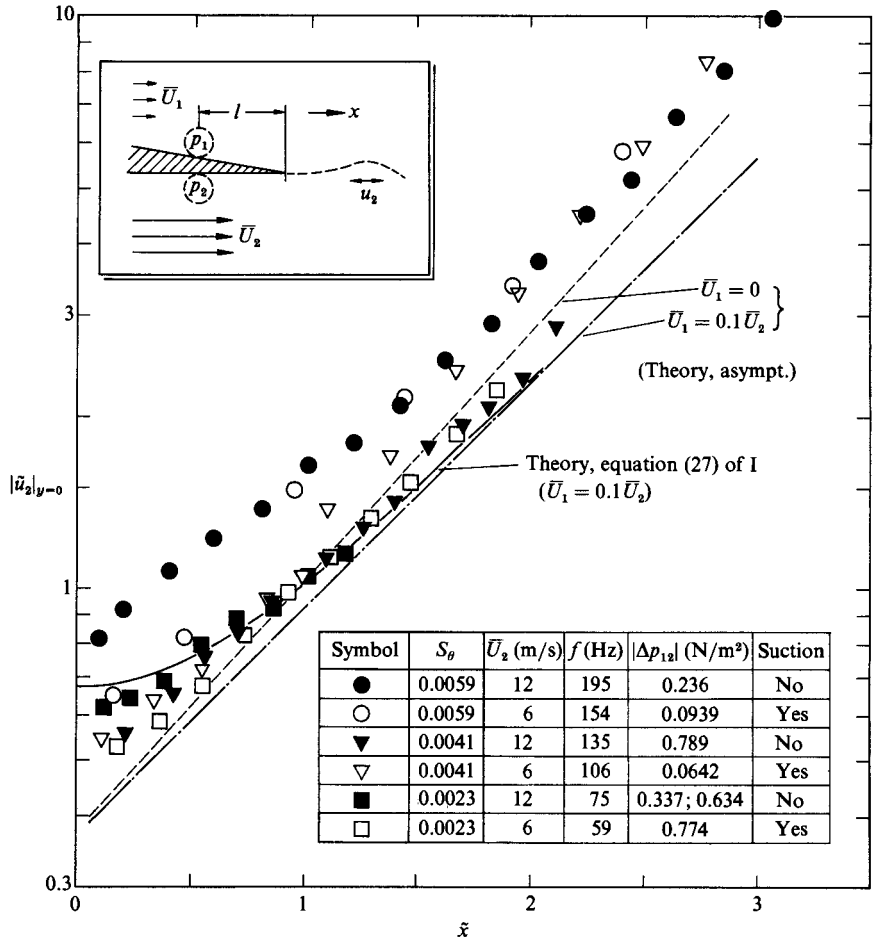

Symbol	S_θ	$\bar{U}_2$ (m/s)	f (Hz)	$\lvert\Delta p_{12}\rvert$ (N/m²)	Suction
●	0.0059	12	195	0.236	No
○	0.0059	6	154	0.0939	Yes
▼	0.0041	12	135	0.789	No
▽	0.0041	6	106	0.0642	Yes
■	0.0023	12	75	0.337; 0.634	No
□	0.0023	6	59	0.774	Yes

FIGURE 11. Shear-layer excitation (data: Berlin 1983/84). Experiments with finite shear-layer thickness θ compared with theory for an infinitesimally thin shear layer. As in figure 10, this diagram shows the dependence of the fluctuation velocity $|\tilde{u}_2|_{y=0}$ on the downstream distance $\tilde{x}$ for various Strouhal numbers S_θ.

of $|u_2|$. Both are original data from the (X, Y)-plotter. The quantity y on the horizontal axis is the perpendicular distance from the centre of the shear layer. The different diagrams represent different locations upstream and downstream of the edge of the splitter plate. The dotted line represents calculated data of $|\tilde{u}_2|$ by Bechert (1982) with $\bar{U}_1 = 0$. The symbol 'TS' (two-stream case) at $y = 0$ stands for the analytic solution (equation (27) of I) of $|u_2|_{(y=-0)}$ for the case where the second stream with $\bar{U}_1 = 0.1\bar{U}_2$ is taken into account. We see that the data are well predicted by the theory. In particular, a discrepancy at small and negative $\tilde{x}$, as suggested by the extrapolated data (figures 10 and 11) does not exist.

The choice of the origin of y may be puzzling at first glance, because $y = 0$, the centre of the shear layer, is not identical with the location of the splitter-plate wall, as required by the theory. The theory is developed only for an infinitesimally thin shear layer and thus both locations are identical there. However, since there are no infinitesimally thin shear layers in reality, we have to live with this conflict. We have chosen as $y = 0$ in figures 12–20 the location in the free-shear layer where $\bar{U}(y)$

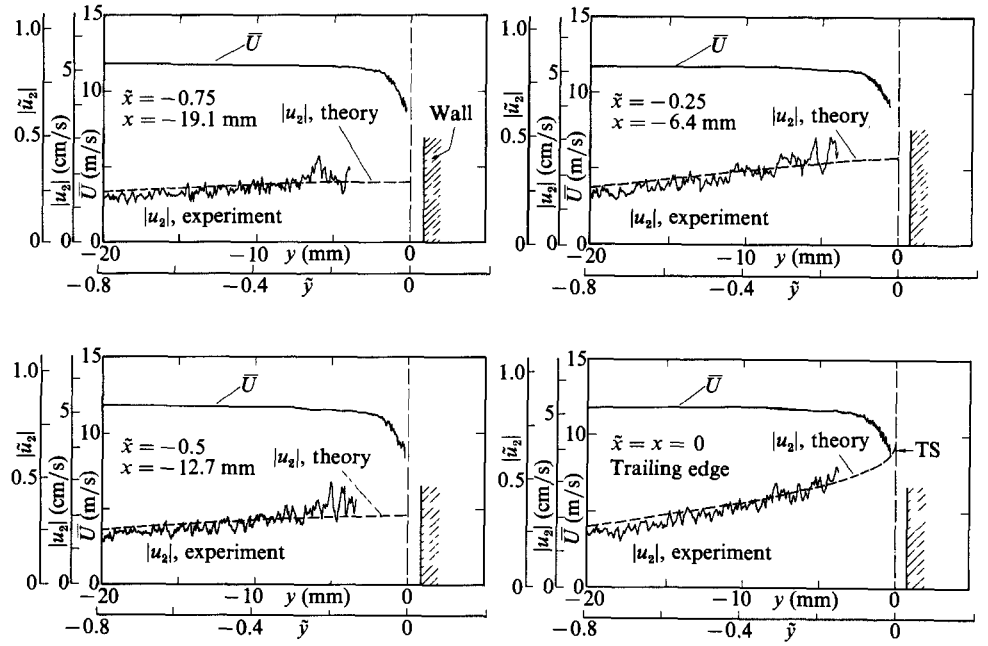

FIGURE 12. Velocity fluctuation $|u_2|$ for varying distance y from the shear layer. The plots show measurements upstream of and at the trailing edge. ——, theory for $\bar{U}_1 = 0$. The experiment is carried out for $\bar{U}_1 = 0.1\bar{U}_2$. For this latter case, the analytic solution at $y = 0$ is given (TS), equation (27) of I. Also, the mean flow $\bar{U}$ is shown. $S_\theta = 0.0023$, $|\Delta p_{12}| = 0.634$ N/m^2, $l = 13$ mm.

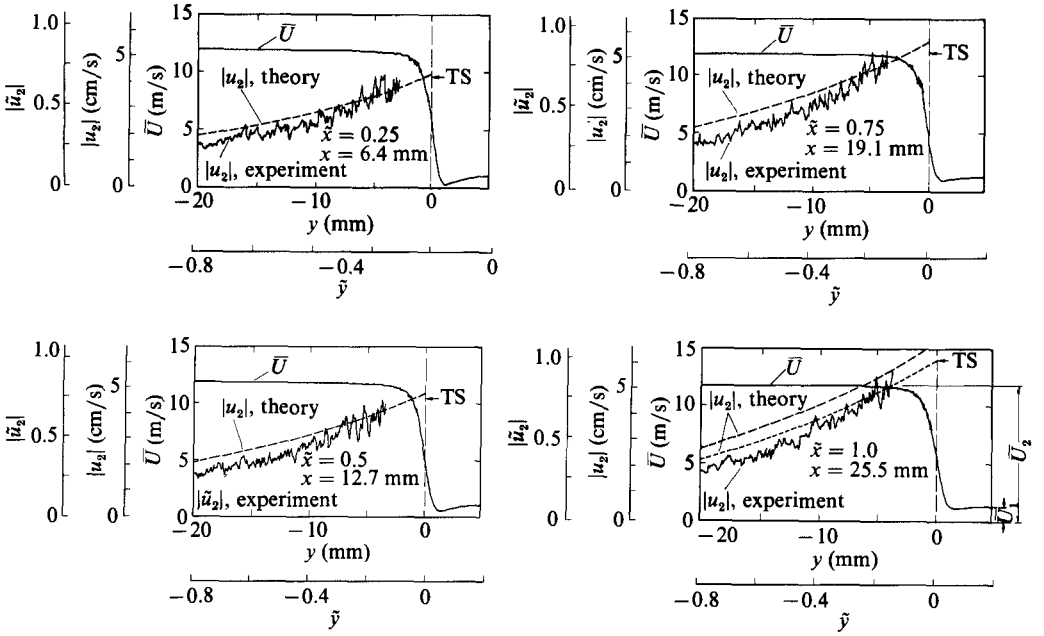

FIGURE 13. Velocity fluctuation $|u_2|$ for varying distance y from the shear layer. The diagrams show different locations downstream of the trailing edge. ---, theory for $\bar{U}_1 = 0$. For $\tilde{x} = 1$ the theory is also extrapolated to include the second stream $\bar{U}_1 = 0.1\bar{U}_2$. 'TS' shows the analytic value at $y = 0$, equation (27) of I. The mean flow is also shown. Other parameters as figure 12.

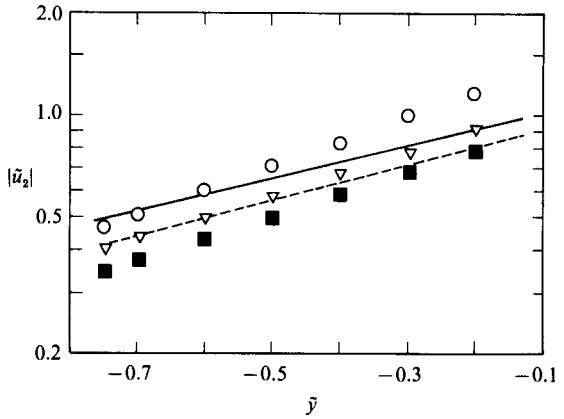

FIGURE 14. Decay rate of the velocity fluctuation $|\tilde{u}_2|$ perpendicular to the shear layer at a downstream distance $\tilde{x} = 1.0$. The Strouhal number S_θ is varied. Experiment: ○, $S_\theta = 0.0053$; ▽, $S_\theta = 0.0041$; ■, S_θ, 0.0023. Theory: ——, $\bar{U}_1/\bar{U}_2 = 0$; – – –, $\bar{U}_1/\bar{U}_2 = 0.1$.

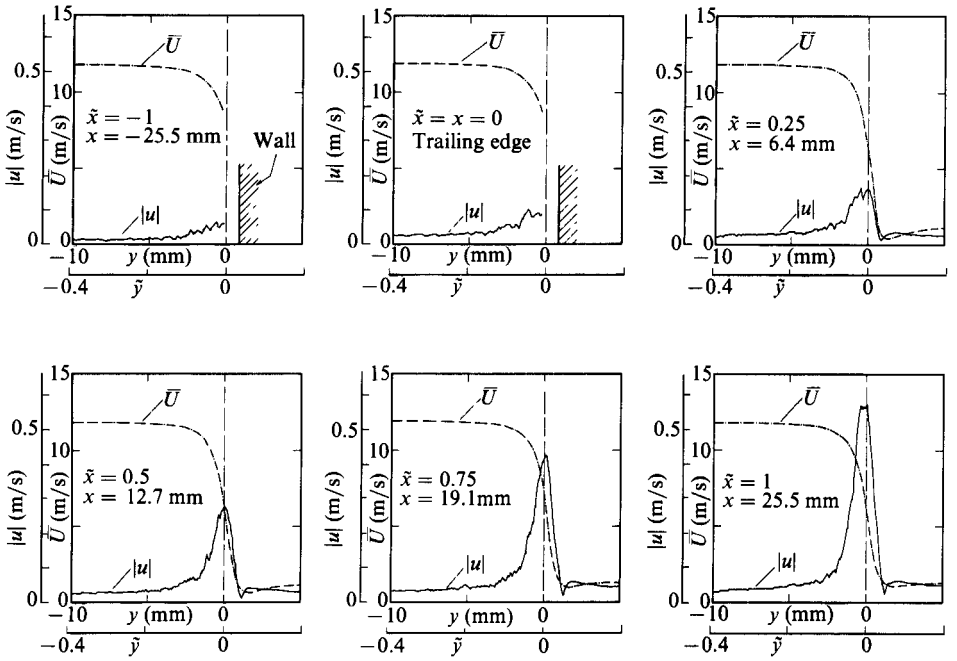

FIGURE 15. Velocity fluctuation in the shear layer for varying x. $S_\theta = 0.0023$. Excitation levels as in figures 12 and 13.

assumes the value $\frac{1}{2}\bar{U}_2$ (see figure 9). We observe also that in cases where the distribution of $|u_2|$ shows a stronger decay in the y-direction, in particular at high Strouhal numbers, an extrapolation to the 'centre' of the shear layer can become arbitrary and meaningless. In our data evaluation, this means that the extrapolation scheme breaks down above, say, $S_\theta \approx 0.007$.

The trend that with increasing Strouhal number the decay of $|u_2|$ in the y-direction is enhanced is worth a little further discussion. In a dimensionless representation, however, with $|\tilde{u}_2|$ plotted versus $\tilde{y}$, this change in the decay rate should be much less

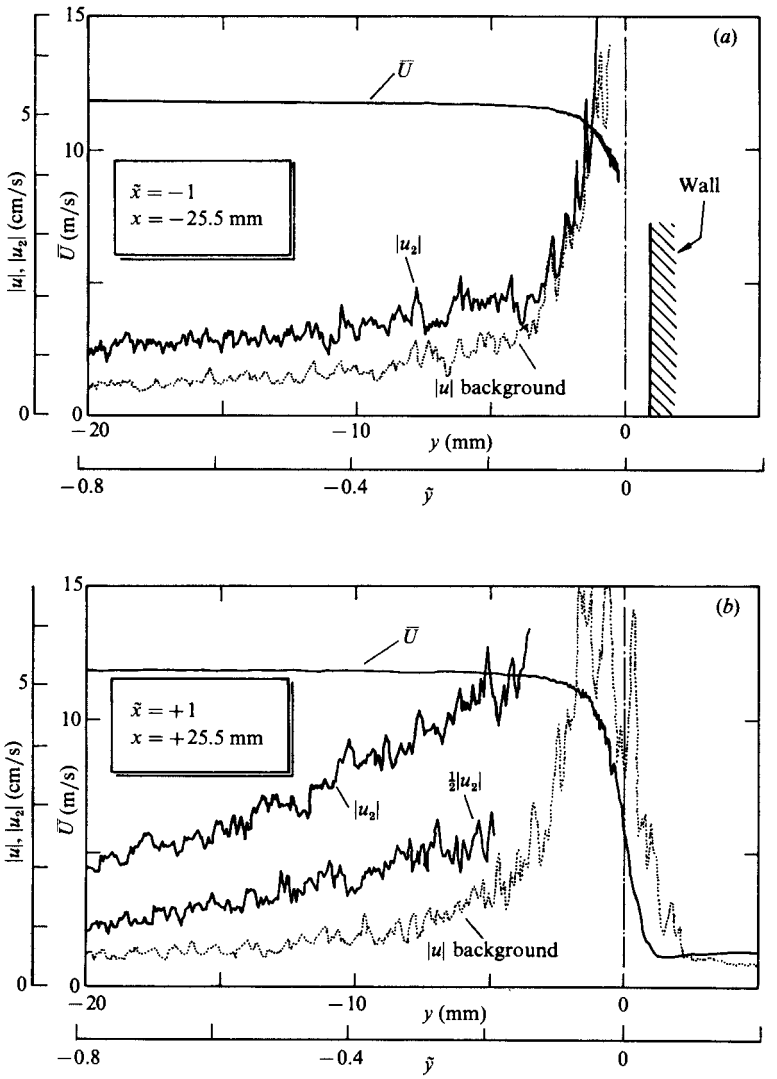

FIGURE 16. Background noise in the fluctuation velocity field compared to the measured signal with tone excitation. The background noise is measured with an r.m.s. meter, but the scale is the same as for the sinusoidal signals, i.e. $2^{\frac{1}{2}}$ times the r.m.s. signal. The measurements are taken (*a*) upstream ($\tilde{x} = -1$) and (*b*) downstream ($\tilde{x} = +1$) of the trailing edge of the splitter plate. The plot at $\tilde{x} = 1$ also shows the linearity of the system by comparing with a fluctuation velocity distribution taken at half the magnitude of the tone excitation. For comparison the mean velocity distribution $\bar{U}$ is also shown. $S_0 = 0.0023$. Excitation levels as in figures 12 and 13.

dramatic. Nevertheless, if we consider figure 5 of I we see that the real wavenumber assumes higher values than the theory of an infinitesimally thin shear layer would predict. This produces higher decay rates in the y-direction. Our measurements basically confirm this, see figure 14.

In figures 12, 13 and 14, only the $|\tilde{u}_2|$-distribution outside the shear layer in the potential-flow region was shown. The development of the $|\tilde{u}|$ fluctuations inside the shear layer is shown in figure 15. We see the evolution of a steep maximum

corresponding to the velocity distribution of the stability calculation of a shear layer with spatial amplification (see Michalke 1965). Upstream of and at the edge of the splitter plate the fluctuation levels are comparatively low. There is no indication of a singularity at the plate edge, which is in agreement with our previous investigations (see Bechert & Pfizenmaier 1975*b*). As we have mentioned earlier, nonlinearities occur first in locations downstream of the plate edge and inside the shear layer. A direct linearity test for $|u_2|$ can be seen in figure 16 in the lower diagram. There, measurements at two different excitation levels are shown. If a doubling of the excitation level produces twice the magnitude of the fluctuation velocities, we can consider the system as linear.

Figure 16 shows also another important feature of such measurements: there is always contamination by background noise. The typical background noise comes from the flow-producing apparatus, i.e. blower, bends, separation and turbulence in the flow-carrying ducts etc. In particular, low-frequency noise below about 100 Hz is very difficult to attenuate by mufflers. In our facilities, we find broadband low-frequency noise without pronounced peaks in the spectrum. However, this noise also excites the shear layer in the same way as our pure-tone excitation does. What we see in figure 16, labelled as 'background' noise, is the narrowband-filtered† signal at the frequency of the excitation, but the excitation is switched off in this case. Uncorrelated background noise begins to become critical for the measurements if it is more than about half ($= -6$ dB) the magnitude of the signal. For -6 dB background-noise contamination, the systematic error becomes 12%. This also has to be kept in mind for the measurement of the excitation level, Δp_{12}. These background-noise problems cannot be avoided: increasing the excitation level decreases the possible downstream range of the measurements, because nonlinearities occur earlier. We see from this example that a low-noise facility, narrowband filtering and a proper adjustment of the excitation level is essential for the quality of the measurements.

Finally, it should be mentioned that the background-noise level in figure 16 is comparatively high, and if it were higher there would be significant errors. In the other measurements, in general, the background-noise contamination is much lower.

5.3. *Phase measurements*

Phase measurements are most crucial to verify the theory. Here the phase of u_2, the fluctuating velocity at $y < 0$, in the mean stream, is measured. The reference phase is that of the excitation pressure difference $\boldsymbol{p}_1 - \boldsymbol{p}_2 = \Delta \boldsymbol{p}_{12}$. Figures 17 and 18 show data sets taken at constant distance y from the shear layer. The phase is plotted versus the downstream location x. The data referred to as 'theory' were interpolated from the computed tables given in Bechert (1982). The phase angle is counted positive if there is a phase lag compared to $\Delta \boldsymbol{p}_{12}$ (which is the same nomenclature as in the tables computed by Bechert 1982). The data were collected in the two different facilities (Houston and Berlin) and at two different Strouhal numbers S_θ. The Berlin data show more jitter due to background noise. The agreement, however, is remarkable. We see only minor discrepancies farther downstream, caused by a slightly lower phase speed than anticipated by the 'thin-shear-layer' theory. This is not unexpected for a shear layer of finite thickness (see figure 5 of I). Near the trailing

† All filtered data are taken with a Brüel & Kjaer 2020 narrowband filter with 3.16 Hz bandwidth.

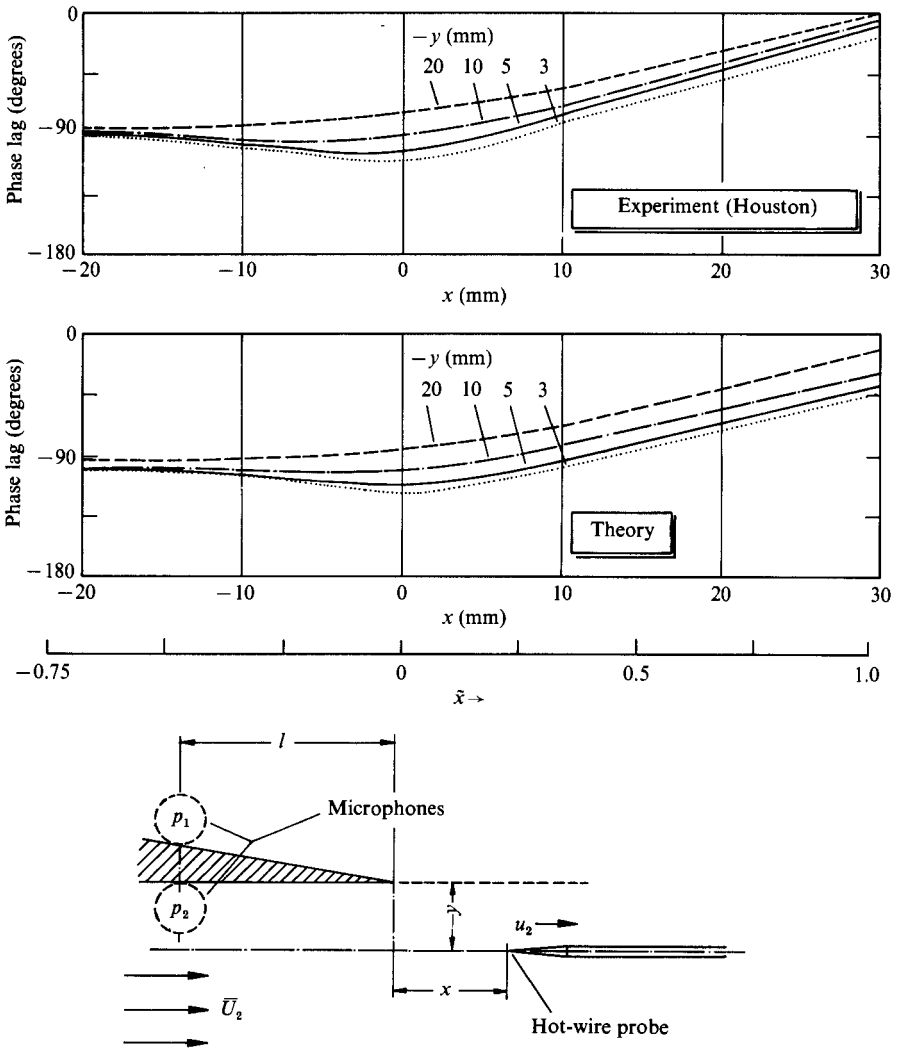

FIGURE 17. Phase measurements of the u_2 velocity fluctuations. The reference phase is the phase of the pressure difference $\Delta p_{12} = p_1 - p_2$. Parameters, dimensional: $\bar{U}_2 = 13.5$ m/s; $f = 82.5$ Hz; $|\Delta p_{12}| = 0.75$ N/m^2; $l = 13$ mm; $\theta = 0.395$ mm; without boundary-layer suction. Parameters, non-dimensional: $S_\theta = 0.0024$

$-y$ (mm)	3	5	10	20
$-\tilde{y}$	0.115	0.192	0.384	0.768

edge, there is a local region of negative phase speed,† as predicted by the theory. This does not indicate negative group speed or any feedback from downstream locations; it is a side effect in the potential field around an excited shear layer.

The general trend of the measurements is quite simple: for negative x, upstream

† We have also already found such local regions of negative phase speed inside the shear layer in previous experiments (see Bechert & Pfizenmaier 1975*b*, *c*). There, the phase measurements were taken at the local $|u|$-maximum location which shifts in its y-position for small distances x from the trailing edge. So the conclusion of having found negative phase speeds had then still some ambiguity in it. For regions farther downstream, however, where the shear layer has developed, the procedure cannot be criticized.

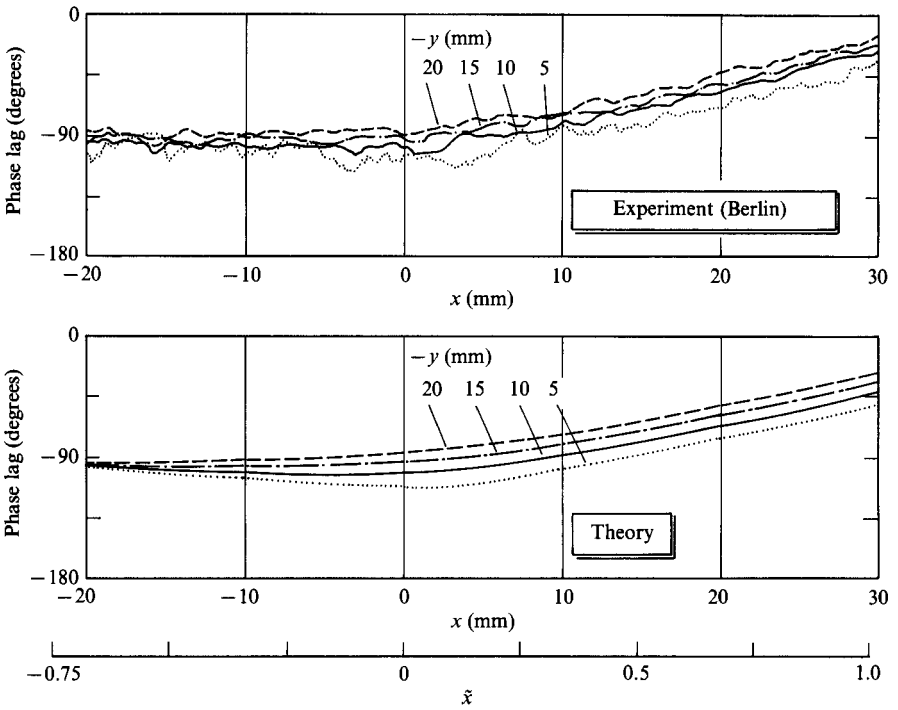

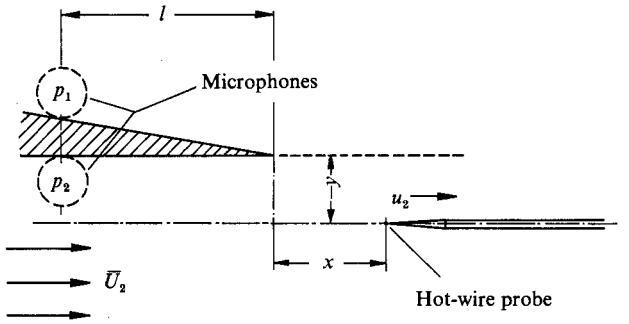

FIGURE 18. Phase measurements of the u_2 velocity fluctuations. The reference phase is the phase of the pressure difference $\Delta p_{12} = p_1 - p_2$. Parameters, dimensional: $\bar{U}_2 = 12$ m/s; $f = 65$ Hz; $|\Delta p_{12}| = 0.75$ N/m^2; $l = 13$ mm; $\theta = 0.225$ mm; with boundary-layer suction. Parameters, non-dimensional: $S_\theta = 0.00122$

$-y$ (mm)	5	10	15	20
$-\tilde{y}$	0.17	0.34	0.51	0.68

of the edge, we find the phase of the excitation field, which dominates there. For regions of positive x, farther downstream of the edge, the instability wave dominates, with a phase speed close to the mean flow speed $\bar{U}_2$. The planes of equal phase are inclined for spatial stability waves. Therefore, we have different phases for different y at constant downstream location x.

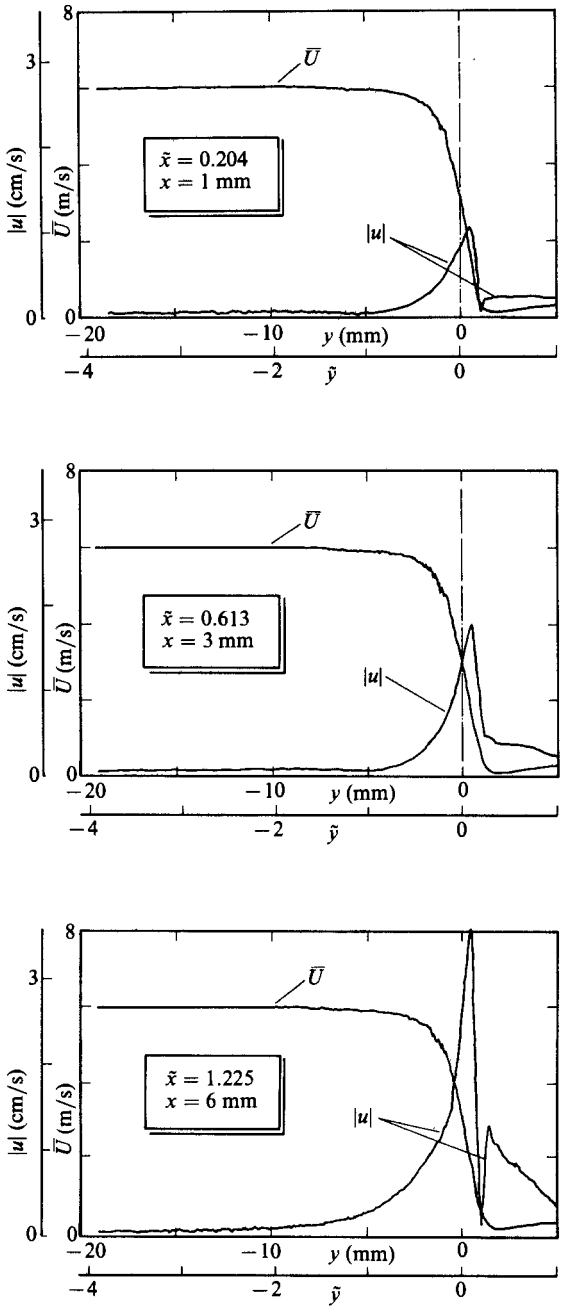

FIGURE 19. Distribution of the $|u|$-velocity fluctuations at higher Strouhal number $S_\theta = 0.0136$, close to the condition of maximum spatial amplification. Excitation pressure difference $\Delta p_{12} = 0.103$ N/m^2, $l = 13$ mm, no boundary-layer suction.

5.4. *Measurements at higher Strouhal numbers*

For higher Strouhal numbers we cannot compare the experimental data with a detailed theory, but some simple considerations provide an understanding of the measurements. The data that we show are obtained at $S_\theta = 0.0136$, close to the

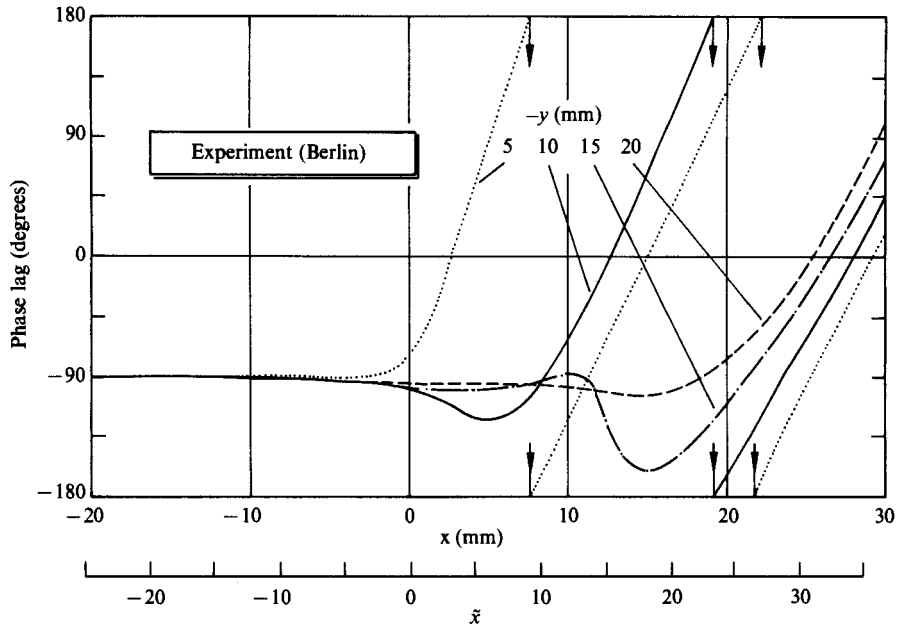

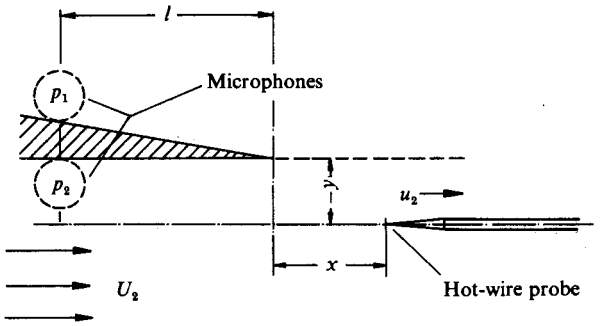

FIGURE 20. Phase measurements of the u_2 velocity fluctuations. The reference phase is the phase of the pressure difference $\Delta p_{12} = p_1 - p_2$. Parameters, dimensional: $\bar{U}_2 = 6$ m/s; $f = 195$ Hz; $|\Delta p_{12}| = 0.103$ N/m^2; $l = 13$ mm; $\theta = 0.42$ mm, without boundary-layer suction. Parameters, non-dimensional: $S_0 = 0.0136$

$-y$ (mm)	5	10	15	20
$-\tilde{y}$	4.08	8.16	12.24	16.32

frequency where maximum amplification occurs (see figure 5 of I). First, we show some fluctuation-magnitude measurements, figure 19. We see that the decay of $|u|$ in the y-direction is so rapid that the decay takes place essentially within the shear layer. The velocities outside the shear layer are produced essentially by the excitation field, which has very low induced $|u|$-levels close to the shear layer. So we find, in particular at small x, a very low $|u|$-level close to the shear layer, which looks almost like a local node.

Figure 20 shows phase measurements at the same Strouhal number. The general

trend is the same as at lower Strouhal numbers: the excitation field and its phase dominate at negative x, upstream of the trailing edge. Far downstream, say at $x >$ 25 mm in our diagram, the instability wave with its tilted wave fronts dominates. The intermediate region looks more puzzling, but is easy to explain. We know that the instability-wave influence decays exponentially for increasing y. So the x-location where the instability wave takes over is different for different y. At $y = -5$ mm, for example, the instability wave takes over just at the trailing edge. For greater distances y, this transition point shifts more towards the downstream direction. The superposition of these two fields produces locally regions of negative phase speed. If we want to extrapolate this trend to even higher Strouhal numbers, we shall find a very detailed local structure like the one Pfizenmaier (1973) found in a jet at very high Strouhal numbers. But we should stress again that the local occurrence of negative phase speeds in our experiments is a consequence of the interaction of propagating shear layer waves and (essentially) standing sound waves. It does not allow the conclusion that these regions are produced by sources located downstream. This is only a warning; we do not deny effects from downstream in general. A discussion on downstream effects, and the conclusion that they are probably weak, is given in I.

6. Conclusions

We have carried out hot-wire and microphone measurements to check our theory of the acoustical excitation of shear layers given in Part I of this work. This theory suggested that the fluctuation field can be split into two constituents: (*a*) the excitation pressure field which is transmitted through the shear layer, and (*b*) the pressure field which, as a reaction, is produced by the shear layer itself. The excitation (*a*) generates an antisymmetrical field close to the splitter-plate edge. Therefore, it produces a pressure difference $|\Delta p_{12}|$ between the two sides of the splitter plate. On the other hand, the field induced by the shear layer (*b*) is symmetrical with respect to the shear layer; hence it does not contribute to the pressure difference $|\Delta p_{12}|$ between the sides of the splitter plate. Consequently, *the pressure difference* Δp_{12} *is the relevant quantity for the acoustical excitation.*† In addition, our previous theory provides numerical data for velocity fluctuation levels and phase angles in the flow field near the plate edge. Moreover, this theory does not contain any empirical constants.

The experiments have been carried out in two similar facilities (Houston 1981 and Berlin 1983/84). The data were taken in the vicinity of the trailing edge of the splitter plate. There, all fluctuating quantities were small and a comparison with the above mentioned linear theory appeared to be meaningful. In addition, the measurements were concentrated on comparatively low Strouhal numbers where a comparison with the theory for a 'thin' shear layer makes sense. Also the so-called large-scale structures in a shear layer correspond to low Strouhal numbers. Therefore, the present investigation may provide some solid background information on how these structures can be generated or enhanced. However, we do not show any of our own flow visualization pictures here because the interaction region near the trailing edge exhibits comparatively low fluctuation levels and hence flow visualization would show an apparently undisturbed laminar flow there.

† Note that $|\Delta p_{12}| = |p_1 - p_2|$ is a difference of two pressures with different modulus and phase. This means that either $|\Delta p_{12}|$ must be measured directly with two microphones or calculated after an independent measurement of the two pressures and their phases, using (2) in §4.

The present measurements are based on (i) a determination of the magnitude of excitation by microphone measurements of the pressure difference Δp_{12} on both sides of the splitter plate, and (ii) hot-wire measurements of the u-fluctuation levels and their phase in the region of the mean flow below the shear layer. The hot-wire measurements are compared with computed theoretical values (see I and Bechert 1982). The agreement between theory and experiment is very encouraging, in particular within the validity range of the 'thin'-shear-layer theory, i.e. for Strouhal numbers $S \leqslant 0.005$.† The measurements confirm even minor details that were predicted by the theory, such as local regions of negative phase speeds of the u-fluctuations. However, these regions of negative phase speeds are independent of upstream effects of sound sources located downstream in the turbulent shear layer. They are only an accurately predicted side effect of the shear-layer excitation.

Finally, we have now experimental evidence of the existence of a Kutta condition for the fluctuating flow of an excited shear layer shed from a trailing edge, valid at least for low Strouhal numbers of up to $S_\theta = 0.005$. This can be concluded from the fact that the measured velocity and phase distributions fit very well the theoretical values calculated for this condition. It also supports the corresponding theoretical considerations given in I.

The theory which is now shown to be valid predicts the fluctuating potential-flow field outside the shear layer. A prediction of the fluctuations inside the shear layer is also possible, at least downstream of the interaction region at the edge. This can be done by adjusting the potential field of our 'thin'-shear-layer theory to the calculated potential field for a shear layer with finite thickness, but infinitely extended in the streamwise direction (see, e.g. Michalke 1965). Thus, the complete perturbation input of a shear layer exposed to a sound field can be predicted. Of course, this statement is only valid for low Strouhal numbers, $S_\theta \leqslant 0.005$, but it may be also useful for estimations at higher Strouhal numbers.

The present work has been sponsored partly by NASA Lewis (Contract NAG 3-198) and by the Deutsche Forschungsgemeinschaft (Contract Be 889/1-1). Most of the equipment used in Berlin comes from earlier DFG contracts, e.g. the vibration systems (Wi 8/35) and the blower as well as the probe traverse hardware (Wi 8/37). The improved electronic instrumentation of the probe traverse was prepared by B. Simon. The authors were encouraged by Professor A. K. M. F. Hussain (University of Houston) to carry out this research. He helped also to arrange for one of the author's (D. W. B.) visit as an associate professor to Houston in this joint U.H.–DFVLR project. We appreciate also the advice of Professor N. Nullschnall and Dr N. Nörgel who helped to establish this paper in the present form.

REFERENCES

Bechert, D. W. 1982 Excited waves in shear layers. *DFVLR-FB* 82-23.

Bechert, D. W. 1983 A model of the excitation of large scale fluctuations in a shear layer. *AIAA paper* 83-0724.

Bechert, D. W. 1988 Excitation of instability waves in free shear layers. Part 1. Theory. *J. Fluid Mech.* **186**, 47–62.

† The Strouhal number appears to be comparatively low. This is due to the definition of S_θ which is calculated with a small quantity, i.e. the momentum thickness, which is much smaller than other typical dimensions of the shear layer. In that context, it is worth mentioning, that the whole range of amplified instability waves of a shear layer is in the range $0 < S_\theta < 0.04$.

BECHERT, D. W. & MICHEL, U. 1975 The control of a thin free shear layer with and without a semi-infinite plate by a pulsating flow field. *Acustica* **33**, 287–307.

BECHERT, D. W. & PFIZENMAIER, E. 1975*a* On the amplification of broad band jet noise by a pure tone excitation. *J. Sound Vib.* **43**, 581–587.

BECHERT, D. W. & PFIZENMAIER, E. 1975*b* Optical compensation measurements on the unsteady exit condition at a nozzle discharge edge. *J. Fluid Mech.* **71**, 123–144.

BECHERT, D. W. & PFIZENMAIER, E. 1975*c* On wavelike perturbations in a free jet travelling faster than the mean flow in the jet. *J. Fluid Mech.* **72**, 341–352.

BECHERT, D. W. & STAHL, B. 1984 Shear layer excitation, experiment versus theory. *DFVLR-FB* 84-26.

CRIGHTON, D. G. & LEPPINGTON, F. G. 1974 Radiation properties of the semi-infinite vortex sheet: the initial value problem. *J. Fluid Mech.* **64**, 393–414.

CROW, S. C. & CHAMPAGNE, F. H. 1971 Orderly structure in jet turbulence. *J. Fluid Mech.* **48**, 547–591.

DENEUVILLE, P. & JAQUES, J. 1977 Jet noise amplification: a practically important problem. *AIAA paper* 77-1368.

DZIOMBA, B. & FIEDLER, H. E. 1985 Effect of initial conditions on two-dimensional free shear layers. *J. Fluid Mech.* **152**, 419–442.

FREYMUTH, P. 1966 On transition in a separated laminar boundary layer. *J. Fluid Mech.* **25**, 683–703.

GUTMARK, E. & HO, C.-M. 1983 Preferred modes and the spreading rates of jets. *Phys. Fluids* **26**, 2932–2938.

LECONTE, J. 1858 On the influence of musical sounds on the flame of a jet of coal-gas. *Lond. Edin. Dub. Phil. Mag.* **15**, 235–239.

MICHALKE, A. 1965 On spatially growing disturbances in an inviscid shear layer. *J. Fluid Mech.* **23**, 521–544.

MICHEL, F. 1932 *Lärm und Resonanzschwingungen im Kraftwerksbetrieb* (Noise and resonant vibrations in power plants). Berlin: VDI–Verlag.†

MÖHRING, W. 1975 On flows with vortex sheets and solid plates. *J. Sound Vib.* **38**, 403–412.

MOORE, C. J. 1977 The role of shear-layer instability waves in jet exhaust noise. *J. Fluid Mech.* **80**, 321–367.

PFIZENMAIER, E. 1973 Zur Instabilität des schallbeeinflußten Freistrahls. *DLR-FB* 73-69. (English transl. On the instability of a sound-influenced free jet. *ESRO TT* 122 (1973).)

RIENSTRA, S. W. 1979 Edge influence on the response of shear layers to acoustic forcing. Ph.D. thesis, University of Eindhoven, Netherlands.

TYNDALL, J. 1867 *Sound*. Longmans.

† The authors owe this reference to Dr A. Dinkelacker, who found this book in L. Prandtl's private library.